# Theoretical study of (Ag,Au and Cu)/$Al_2O_3$ interfaces



2009 J. Phys.: Condens. Matter 21 315003

(http://iopscience.iop.org/0953-8984/21/31/315003)

J. Phys.: Condens. Matter **21** (2009) 315003 (8pp) doi:10.1088/0953-8984/21/31/315003

# Theoretical study of (Ag, Au and Cu)/$Al_2O_3$ interfaces

**Y Long**[1,2] **and N X Chen**[1,3]

[1] Department of Physics, Tsinghua University, Beijing 100084, People's Republic of China
[2] Center for Advanced Study, Tsinghua University, Beijing 100084, People's Republic of China
[3] Institute for Applied Physics, University of Science and Technology, Beijing 100083, People's Republic of China

E-mail: longyao@tsinghua.org.cn

Received 28 December 2008, in final form 8 June 2009
Published 19 June 2009
Online at stacks.iop.org/JPhysCM/21/315003

**Abstract**

Interface structure is a basic problem in interface and surface science. It is usually indicated by atomic positions for an ideal interface. But this way is sometimes unsuitable for a mismatch interface, because there are too many atoms under consideration, whose coordinates may confuse our mind in understanding the interface structure. In this case, a 'dislocation representation' is introduced. A misfit dislocation network is used as an effective representation of the interface structure. However, there are two questions on this topic. How to determine the dislocation network structure? And how to relate it to interface dynamics? In this paper, we work on the first question and make an effort to build up the 'dislocation representation' for metal/$Al_2O_3$ interfaces.

(Some figures in this article are in colour only in the electronic version)

## 1. Introduction

The metal/oxide interface is an important issue in surface and interface science. It has many applications in catalysts, composite materials, metal–ceramic sensors, etc [1–4], and so it attracts attention. The interface structure, adhesion, segregation, wetting and misfit dislocation are most widely studied topics [5–7], usually by *ab initio* and atomistic methods [8–13].

In this work, we are interested in (Ag, Au and Cu)/$Al_2O_3$ (0001) interfaces and on their characterization method. For an ideal interface, an 'atomic representation' is used. The interface structure is confirmed by atomic positions. But for a mismatch interface, this way is sometimes unsuitable, as the effective interface area is quite large. So we use a 'dislocation representation', and take a dislocation network (DN) as the basic frame for interface structure, instead of specific atomic configurations.

In previous works, we have already studied the Ni/$Al_2O_3$ interface on the DN's structure [14, 15]. The present work also includes this topic, but goes far beyond it. Misfit dislocation is considered in a new way—the 'dislocation representation'.

For misfit dislocation, the Burgers vector is an important issue. Usually, it is equal to the smallest lattice vector. In bcc-metal/$Al_2O_3$(0001) interfaces, it is $\frac{a_M}{2}[111]$ [16, 17], where $a_M$ is the lattice constant (M = Ag, Au or Cu), see table 1. But in fcc-metal/$Al_2O_3$(0001) interfaces of interest in this work, it can be $\frac{a_M}{2}[1\bar{1}0]$ and $\frac{a_M}{2}[0\bar{1}\bar{1}]$ in principle. The former one is parallel to the interface and the latter one is not parallel. In experiments, just $\frac{a_M}{2}[1\bar{1}0]$ has been reported for Cu/$Al_2O_3$ [18]. But following the bcc-metal/$Al_2O_3$'s result, $\frac{a_M}{2}[0\bar{1}\bar{1}]$ is also considered in this work.

**Table 1.** Lattice constants and misfits of (Ag, Au and Cu)/$Al_2O_3$ interfaces, where $a_M$ is from theoretical calculation in this work, and $a_{Al_2O_3}$ and $c_{Al_2O_3}$ are experimental values [23].

| | $a_M$ (Å) | $\gamma_0$ |
|---|---|---|
| Ag | 4.141 | −6.16% |
| Au | 4.168 | −6.77% |
| Cu | 3.626 | 7.16% |
| $Al_2O_3$ | $a_{Al_2O_3} = 4.759$ Å, $c_{Al_2O_3} = 12.989$ Å | |

Now, let us present some background information on these interfaces. First, the misfit across the interface is

$$\gamma_0 = \frac{\sqrt{\frac{2}{3}}a_{Al_2O_3} - a_M}{a_M} \quad (1)$$

 

**Table 2.** Potential parameters of $\Phi_{Ag-O}$, $\Phi_{Ag-Al}$, $\Phi_{Au-O}$, $\Phi_{Au-Al}$, $\Phi_{Cu-O}$ and $\Phi_{Cu-Al}$.

| | $D_0$ (eV) | $R_0$ (Å) | $y$ | $a_1$ (eV) | $b_1$ (Å$^{-1}$) | $c_1$ (Å) | $a_2$ (eV) | $b_2$ (Å$^{-1}$) | $c_2$ (Å) | $a_3$ (eV) | $b_3$ (Å$^{-1}$) | $c_3$ (Å) |
|---|---|---|---|---|---|---|---|---|---|---|---|---|
| $\Phi_{Ag-O}$ | 103.63 | 1.00 | 1.75 | −44.25 | 3.08 | 1.47 | −24.77 | 1.86 | 2.11 | 3.50 | 2.26 | 2.62 |
| $\Phi_{Ag-Al}$ | 5.55 | 1.00 | 1.61 | −24.27 | 2.43 | 1.85 | 63.38 | 2.28 | 1.38 | −0.41 | 2.19 | 3.59 |
| $\Phi_{Au-O}$ | 125.36 | 1.00 | 2.17 | −101.23 | 2.31 | 1.23 | −1.04 | 1.89 | 2.88 | 3.18 | 1.73 | 1.79 |
| $\Phi_{Au-Al}$ | 72.31 | 1.00 | 2.20 | −32.57 | 1.69 | 1.47 | 0.38 | 3.22 | 2.98 | 24.01 | 1.47 | 0.99 |
| $\Phi_{Cu-O}$ | 61.24 | 1.00 | 1.86 | −64.36 | 2.13 | 1.34 | 6.66 | 2.48 | 1.87 | −0.33 | 1.73 | 3.27 |
| $\Phi_{Cu-Al}$ | 181.76 | 1.00 | 2.93 | −60.05 | 2.33 | 1.46 | −29.71 | 7.75 | 1.45 | 11.01 | 2.48 | 2.10 |

where $a_{Al_2O_3}$ is the lattice constant of $Al_2O_3$, also listed in table 1. Note that $\gamma_0$ is positive for $Cu/Al_2O_3$ and negative for (Ag and Au)/$Al_2O_3$. This may lead to different structural and energetic properties on misfit dislocations. Then, $Cu/Al_2O_3$ is widely studied in experiments [18, 19], while (Ag and Au)/$Al_2O_3$ are limited in theoretical calculations [20–22]. In our mind, the former one can suggest some experimental checks and the latter two are predictions.

The following work consists of four parts. First, in section 2, we introduce the interatomic potentials for atomistic simulation. Then, in section 3, an ideal interface is studied by using the 'atomic representation'. Next, in section 4, the misfit dislocation is considered for the mismatch interface. The dislocation structure, position, energy and Burgers vector are calculated, resulting in the 'dislocation representation'. Finally, section 5 is the conclusion.

## 2. Interatomic potentials

The interatomic potential is a prerequisite for all kinds of atomistic simulations. Its determination is usually a challenging problem. In previous works, we have used a Chen–Möbius inversion method to get a series of parameter-free potentials, and checked them over a wide range [14, 24–26]. Now, we use them again for advanced studies.

In general, metal/alumina interfaces contain three kinds of atomic interactions: metal–metal, alumina–alumina and metal–alumina pairs. The former two are inner bulk materials and the latter one is across the interface. Each of them is introduced below.

First, metal–metal potentials have been presented in our previous work [27], so we do not say anymore here. Then, metal–alumina potentials are obtained by the inversion method mentioned above [14]. A series of checks show that they are quite applicable for Al-terminated interfaces, but not O-terminated interfaces. So we just consider Al-terminated cases in this work (or briefly, M/$(Al_2O_3)_{Al}$, M = Ag, Au and Cu). The potential function is of the Rahman–Stillinger–Lemberg form:

$$\Phi = D_0 e^{y(1-\frac{r}{R_0})} + \frac{a_1}{1+e^{b_1(r-c_1)}} + \frac{a_2}{1+e^{b_2(r-c_2)}} + \frac{a_3}{1+e^{b_3(r-c_3)}}. \quad (2)$$

The potential parameters are listed in table 2

Finally, alumina–alumina potentials are ignored in this work because all the potentials we have found for $Al_2O_3$ cannot keep a stable Al-terminated interface. It always changes to an O-terminated one after atomic relaxation. In this condition, we take $Al_2O_3$ as a rigid body and ignore its inner interactions. It is surely a primary approximation for atomistic simulation, but sometimes reasonable, as $Al_2O_3$ is more rigid than metal. In particular, fixing the $Al_2O_3$ body can greatly reduce the free variables in calculation and helps us go to a large scale.

**Table 3.** Lattice energy parameters and surface energies of Ag, Au and Cu, obtained by atomistic calculations.

| | $\varepsilon_0$ (eV) | $\varepsilon_2$ (eV) | $\varepsilon_3$ (eV) | $\sigma$ (eV Å$^{-2}$) |
|---|---|---|---|---|
| Ag | −2.80 | 28.30 | −98.88 | 0.17 |
| Au | −3.24 | 42.96 | −198.19 | 0.15 |
| Cu | −3.82 | 26.79 | −99.81 | 0.34 |

## 3. Ideal interface

Now, we are going to study an ideal interface. As we have mentioned above, 'atomic representation' is used in this section by considering atomic positions. The preferred interface structure is picked out from a series of possible cases by the lowest energy principle. Atomistic calculations are performed by the Cerius$^2$ program [28].

Before the main part, some important issues are presented. First, the total energy of an interface system contains many parts, including surface energy, interface energy, lattice energy, etc. The interface energy is obtained by subtracting all the other parts from the total energy:

$$\sigma_{M/Al_2O_3} = \frac{E_{total} - n\varepsilon}{S} - \sigma \quad (3)$$

where $E_{total}$ is total energy, $\sigma$ and $\varepsilon$ are surface and lattice energies of metal layers, and $n$ is the number of metal atoms. Note that $Al_2O_3$ is a rigid body, and has no energy term. Otherwise, the interface is built up by putting metal layers on $Al_2O_3$, resulting in an extra metal surface on the top side. So surface energy is taken into account. Its value is listed in table 3.

As we see, $\sigma_{M/Al_2O_3}$ is obtained by subtracting lattice and surface energies from the total energy. For an ideal interface, it is just the interface energy (see table 5). But if misfit dislocation is taken into account (as we will do in section 4), the result contains both the interface energy and dislocation energy. So for distinction, we use $\sigma'_{M/Al_2O_3}$ instead of $\sigma_{M/Al_2O_3}$ in this case. There is a relation

$$\sigma'_{M/Al_2O_3} = \sigma_{M/Al_2O_3} + \rho e_{dis} \quad (4)$$

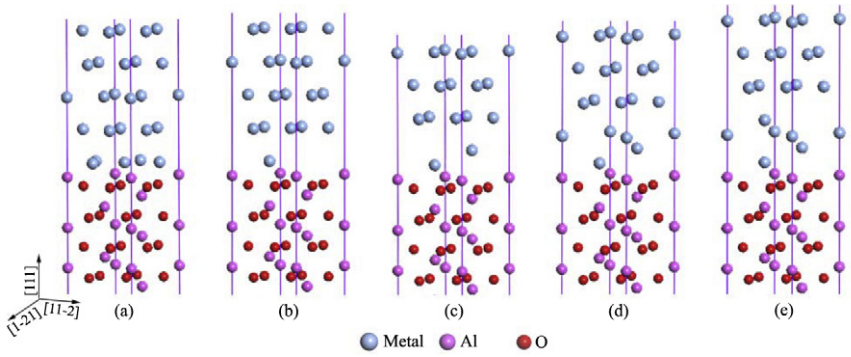


**Figure 1.** Some possible structures for ideal interface. (a) The first layer is reconstructed. (b)–(d) There are $\frac{1}{3}$–$\frac{4}{3}$ translation layers.

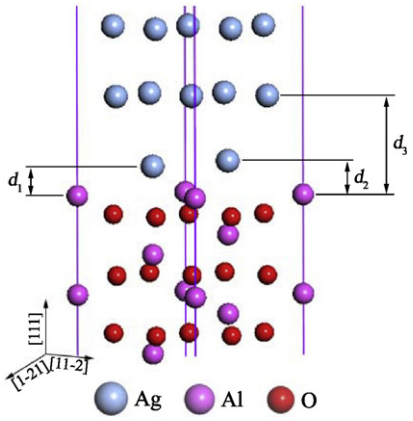


**Figure 2.** Optimized structure of $Ag/Al_2O_3$.

where $e_{dis}$ is dislocation energy per unit length and $\rho$ is dislocation density, which is equal to the length of dislocation lines (DLs) in unit area.

To our mind, misfit dislocation is also a kind of interface relaxation. It concentrates misfits to DLs and makes other parts coherent. So $\sigma'_{M/Al_2O_3}$ is a generalized interface energy for the mismatch interface, while $\sigma_{M/Al_2O_3}$ is just for the ideal interface, although both of them are calculated by the same formula (4).

Second, lattice energy $\varepsilon$ is a variable of metal deformation in this work, which is determined by misfit strain. As we known, misfit dislocations can reduce this strain, but it always remains a little. For quantitative evaluation, we define a residual misfit

$$\gamma = \gamma_0 - \tfrac{1}{2}\rho b_\perp \tag{5}$$

where $b$ is the Burgers vector and $b_\perp$ is its normal component to the DL. Usually, the $\pm$ of $b_\perp$ is consistent with $\gamma_0$, to make $|\gamma| < |\gamma_0|$. So for (Ag and Au)/$Al_2O_3$, $b_\perp < 0$, and for Cu/$Al_2O_3$, $b_\perp > 0$. In particular, if $\gamma = 0$, the metal part is undeformed and $\varepsilon$ achieves its lowest value. We can get $\frac{d\varepsilon}{d\gamma}|_{\gamma=0} = 0$.

Based on the above discussions, $\varepsilon$ is a function of $\gamma$. It can be written as a Taylor expansion:

$$\varepsilon = \varepsilon_0 + \varepsilon_2\gamma^2 + \varepsilon_3\gamma^3 \tag{6}$$

**Table 4.** The values of $d_1$, $d_2$ and $d_3$ for (Ag, Au and Cu)/$Al_2O_3$.

| | $d_1$ (Å) | $d_2$ (Å) | $d_3$ (Å) |
|---|---|---|---|
| $Ag/Al_2O_3$ | 1.06 | 1.24 | 3.65 |
| $Au/Al_2O_3$ | 1.09 | 1.27 | 3.67 |
| $Cu/Al_2O_3$ | 0.54 | 0.85 | 2.78 |

where $\varepsilon_0$, $\varepsilon_2$ and $\varepsilon_3$ are undetermined parameters. The first-order term is ignored, because $\frac{d\varepsilon}{d\gamma}|_{\gamma=0} = 0$. In principle, $\varepsilon_0$ is equal to sublimation heat, $\varepsilon_2$ is related to second-order elastic constants and $\varepsilon_3$ is related to third-order elastic constants. For convenience, we use atomistic calculations to get all of them, as listed in table 3. Note that $\varepsilon_3$ is always negative. It means metals are easy to stretch than to compress.

Now, let us proceed to the main part of this section—the optimized structure of (Ag, Au and Cu)/$Al_2O_3$ interfaces. For this purpose, we consider a series of possible structures with different kinds of reconstruction or translation layers on the interface, as shown in figure 1. Among them, figure 1(a) follows Ni/$Al_2O_3$'s result in [15], which contains a reconstructed layer. Then figures 1(b)–(d) have $\frac{1}{3}$ to $\frac{4}{3}$ translation layers.

Atomistic calculations show that figure 1(c) has the lowest interface energy (see figure 2 of its optimized structure). The $\frac{2}{3}$ metal layer mixes with the Al-terminated layer and forms a new translation layer. For the discussion, Al in $Al_2O_3$ is much sparser than it is in pure metal. So there are many vacancies between Al ions. In bulk $Al_2O_3$, they are filled by O ions. But on the Al-terminated interface, they can just be filled by metal atoms, resulting in a mixed layer.

In summary, the three interfaces (Ag, Au and Cu)/$Al_2O_3$ have a similar optimized structure, just different in geometric parameters, as illustrated in figure 2. There are three parameters for this geometry: $d_1$, $d_2$ and $d_3$. Among them, $d_1$ and $d_2$ are vertical distances between metal atoms and Al ions in the mixed layer and $d_3$ is the distance between the mixed layer and the next metal layer. Table 4 shows their values. As $d_3$ is much larger than $d_1$ and $d_2$, the first $\frac{2}{3}$ metal layer and the Al-terminated layer are close enough to form a new translation layer.

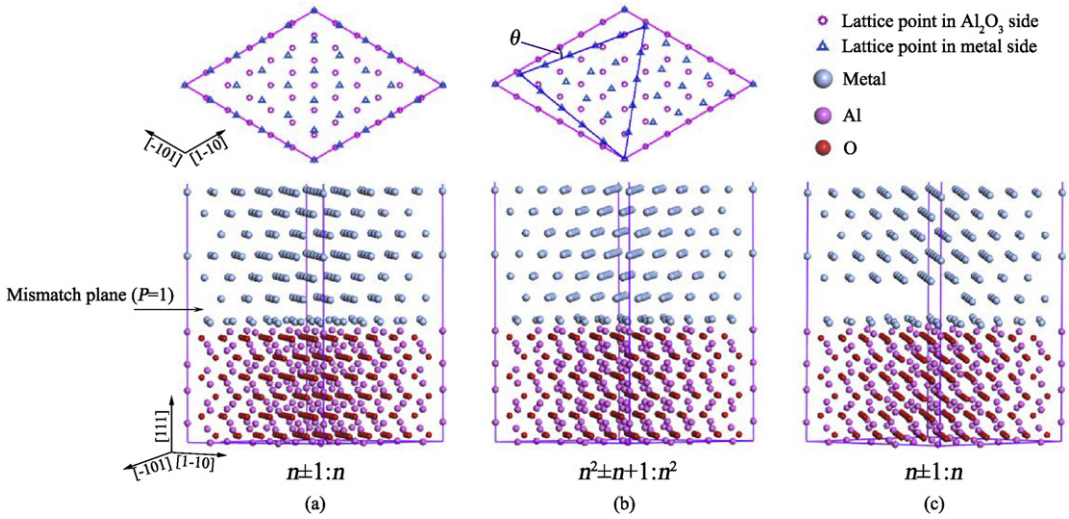


**Figure 3.** Possible structures for mismatch interface. (a) $b \perp$ DL, (b) $b \not\perp$ DL, (c) $b \nparallel Al_2O_3(0001)$.

**Table 5.** The values of $\sigma_{M/Al_2O_3}$ and $e_{dis}$ for (Ag, Au and Cu)/$Al_2O_3$ interfaces.

| | | $b$ | $e_{dis}$ (eV Å$^{-1}$) | $\sigma_{M/Al_2O_3}$ (eV Å$^{-2}$) |
|---|---|---|---|---|
| Ag/$Al_2O_3$ | $b \perp$ DL | $\frac{a_M}{2}[1\bar{1}0]$ | −1.3892 | 0.1442 |
| | $b \not\perp$ DL | $\frac{a_M}{2}[1\bar{1}0]$ | −0.2396 | 0.1229 |
| Au/$Al_2O_3$ | $b \perp$ DL | $\frac{a_M}{2}[1\bar{1}0]$ | −1.5099 | 0.1814 |
| | $b \not\perp$ DL | $\frac{a_M}{2}[1\bar{1}0]$ | −0.1915 | 0.1412 |
| Cu/$Al_2O_3$ | $b \perp$ DL | $\frac{a_M}{6}[2\bar{1}\bar{1}]$ | 1.0061 | 0.0150 |
| | $b \not\perp$ DL | $\frac{a_M}{2}[1\bar{1}0]$ | 0.6655 | −0.0022 |

## 4. Mismatch interface

In section 3, the ideal interface has been studied. It is quite simple, because we just need to consider a small interface area. Now, the mismatch interface is taken into account. A large interface area makes it sometimes complex. So 'atomic representation' is unsuitable. In this section, we choose another way to achieve the interface structure, called the 'dislocation representation'. Atomistic calculations also use the Cerius$^2$ program [28].

### *4.1. Methodology*

As we have mentioned in section 1, the Burgers vector in the fcc-metal/$Al_2O_3$ interface is more complex than in bcc-metal/$Al_2O_3$. It can be $\frac{a_M}{2}[1\bar{1}0]$ or $\frac{a_M}{2}[0\bar{1}\bar{1}]$. The former is parallel to the interface ($b \parallel Al_2O_3(0001)$), but the latter one is not parallel ($b \nparallel Al_2O_3(0001)$).

For the multiplicity of the Burgers vector, we consider three kinds of interface configurations, as shown in figure 3. Among them, figures 3(a) and (c) have a $n\pm1{:}n$ ratio across the mismatch plane and figure 3(b) has a $n^2 \pm n + 1{:}n^2$ ratio, where $\pm$ is for positive or negative misfit. The latter one includes a small angle between M[$1\bar{1}0$] and $Al_2O_3$[$11\bar{2}0$], as shown in (7). By the way, figure 3(a) is $b \perp$ DL, figure 3(b) is $b \not\perp$ DL and figure 3(c) is $b \nparallel Al_2O_3(0001)$.

$$\theta = \arcsin\frac{\sqrt{3}}{2n}. \tag{7}$$

Then let us consider the possible DNs and Burgers vectors for the above interfaces. First of all, figures 3(b) and (c) just have a unique DN in trigonal structure, with $b = \frac{a_M}{2}[1\bar{1}0]$ and $\frac{a_M}{2}[0\bar{1}\bar{1}]$, respectively, as illustrated in figures 4(b) and (c). Then, figure 3(a)'s DN can be hexagonal or trigonal, with $b = \frac{a_M}{2}[1\bar{1}0]$ or $\frac{a_M}{6}[2\bar{1}\bar{1}]$, see figures 4(a.1) and (a.2). In particular, figure 4(a.2) has stacking faults on the interface, which has been shown in Ernst's review [29].

### *4.2. Dislocation position*

Now, we pay attention to dislocation position ($P$). In this work, it is equal to the mismatch plane's position in the initial model, as illustrated in figure 3(a) for the case of $P = 1$. In general, there are two tendencies for $P$. First, misfit dislocation can relax misfit strain and $P - 1$ is equal to the number of unrelaxed monolayers (MLs). So $P$ tends to 1 to reduce the strain energy. Second, the interface effect can change the dislocation structure, and may get a larger dislocation energy than in bulk metal. So $P$ may tend to $\infty$ to reduce this energy term. Considering these opposite parts, we perform some calculations.

First of all, we prove that the interface structure in figure 3(c) ($b \nparallel Al_2O_3(0001)$) cannot be stable in atomic relaxation, as shown in figure 5. It becomes confusing after energy optimization, no matter (Ag, Au and Cu)/$Al_2O_3$. However, this is different from bcc-metal/$Al_2O_3(0001)$ [16, 17], in which only $b$ can be $\frac{a_M}{2}[1\bar{1}0]$, not parallel to the interface plane. So in the following work, we just consider figures 3(a) and (b) as possible structures.

Then, we use the lowest energy principle to determine $P$. Due to the modeling method in figure 3, the number of metal atoms ($n$) is changed for dislocation at different layers. So in order to evaluate $P$, the energy term associated with $n$ must be

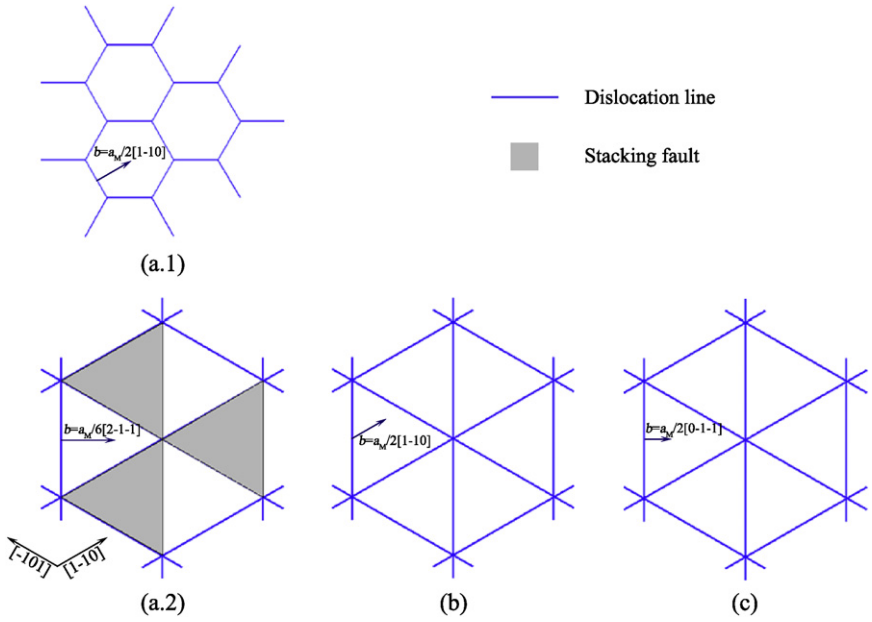


**Figure 4.** Possible Burgers vectors and DNs for figures 3(a)–(c).

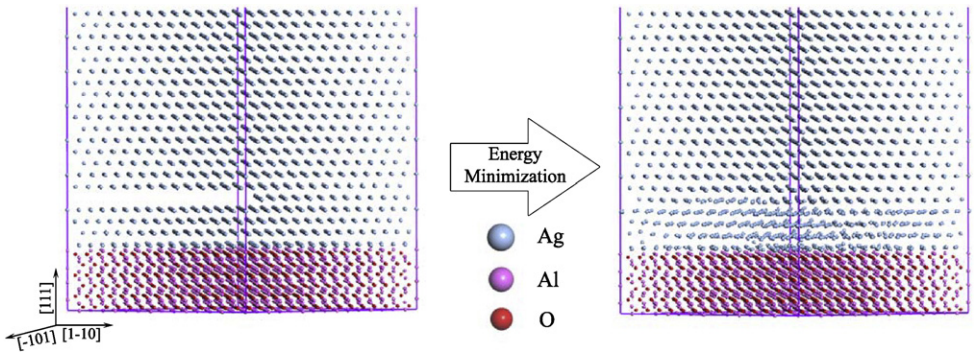


**Figure 5.** Atomic relaxation of $Ag/Al_2O_3$ in figure 3(c), $P = 4$.

subtracted from the total energy, just as we have done in (3). It means that the generalized interface energy $\sigma'_{M/Al_2O_3}$ from (3) can be used as the criterion in this subsection.

As a result, we get $\sigma'_{M/Al_2O_3}$ after atomic relaxation, as shown in figure 6. The calculation covers (Ag, Au and Cu)/$Al_2O_3$, for $P = 1$–5. It shows $P = 1$ is the lowest energy position, no matter $b \perp$ DL or $b \not\perp$ DL.

### *4.3. Dislocation network*

The purpose of this subsection is to determine the DN from figures 4(a.1) and (a.2) at $b \perp$ DL. For $b \not\perp$ DL, the DN is unique, not considered now.

From the above discussions, (Ag, Au and Cu)/$Al_2O_3$ have a translation layer on the interface, so we cannot find a Burgers circuit across the interface to confirm the DL. In order to get the DN, strain distribution is taken into account, just as we have done before [15]. In this view, the DN occupies the strain concentration area, and the other parts are the interface coherent area.

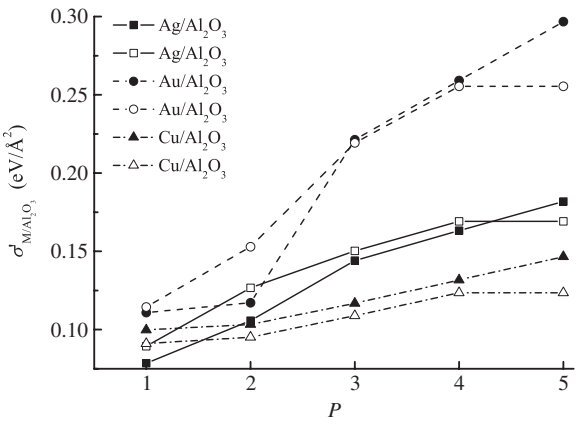


**Figure 6.** $\sigma'_{M/Al_2O_3}$ for (Ag, Au and Cu)/$Al_2O_3$, $P = 1$–5.

Figure 7 displays the calculated strain distribution on (Ag and Cu)/$Al_2O_3$ interfaces, indicated by M–M distances (M = Ag and Cu now). Au/$Al_2O_3$ is ignored because it is similar to $Ag/Al_2O_3$.

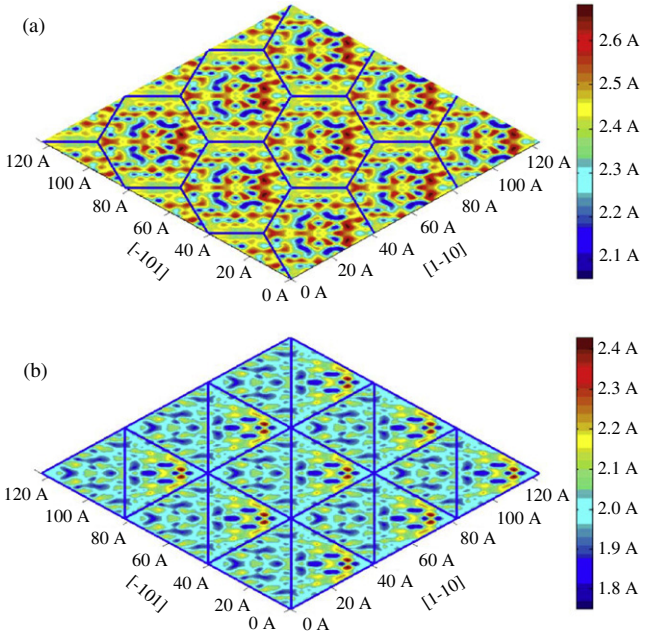


**Figure 7.** M–M distance distribution on (a) $Ag/Al_2O_3$ and (b) $Cu/Al_2O_3$ interfaces.

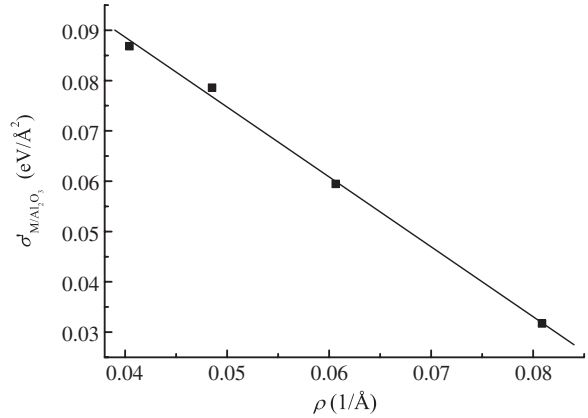


**Figure 8.** The $\sigma'_{M/Al_2O_3}$ versus $\rho$ curve for $Ag/Al_2O_3$ interface in the case of $b \perp$ DL.

As a result, we see that in the case of $b \perp$ DL, the DN is hexagonal for $Ag/Al_2O_3$ (also for $Au/Al_2O_3$, in figure 4(a.1)) and trigonal for $Cu/Al_2O_3$ (in figure 4(a.2)), with $b = \frac{a_M}{2}[1\bar{1}0]$ and $\frac{a_M}{6}[2\bar{1}\bar{1}]$.

### *4.4. Dislocation energy and density*

As dislocation position and network have been confirmed, we now pay attention to dislocation energy $e_{dis}$. From (4), it is a part of the generalized interface energy $\sigma'_{M/Al_2O_3}$. As the latter is available in atomistic calculations (by using (3)), $e_{dis}$ can be fitted from the $\sigma'_{M/Al_2O_3}$ versus $\rho$ curve, as shown in figure 8. From this figure, the good linearity between $\sigma'_{M/Al_2O_3}$ and $\rho$ proves that (4) is reasonable.

Resultant values of $\sigma_{M/Al_2O_3}$ and $e_{dis}$ are listed in table 5. It is worth noting that $e_{dis}$ is negative for (Ag and Au)/$Al_2O_3$ and positive for $Cu/Al_2O_3$, which is consistent with the misfit (in table 1). In general, dislocation is a line defect in materials. It induces lattice distortion, so increases the total energy. In this view, dislocation energy is positive in bulk metals. But on the interface it can be negative in some cases.

For a discussion, note that the DN is a kind of interface relaxation and dislocation energy is included in $\sigma'_{M/Al_2O_3}$ (see (4)). We use a variable

$$\delta\gamma = \frac{\sqrt{\frac{2}{3}}a_{Al_2O_3} - a'_M}{a_M} \tag{8}$$

to denote this relaxation, where $a'_M$ is the distorted lattice constant. Obviously, $\delta\gamma$ tends to 0 on the coherent area.

Due to the definition of Burgers vector, we can get

$$\int_S \delta\gamma \, dS = -\tfrac{1}{2}\rho b_\perp \tag{9}$$

where $S$ is the interface area and $b_\perp$ has been mentioned in (5).

As $Al_2O_3$ is a rigid body now, interface relaxation is limited on the metal side. So dislocation energy is an integral of the surface relaxation energy ($\delta\sigma$) on M(111) (M = Ag, Au or Cu):

$$e_{dis} = \frac{1}{\rho}\int_S \delta\sigma \, dS. \tag{10}$$

Following the lattice energy's formula (6), $\delta\sigma$ can also be written as

$$\delta\sigma = \sigma_2\delta\gamma^2 + \sigma_3\delta\gamma^3. \tag{11}$$

Obviously, surface energy parameters $\sigma_2$ and $\sigma_3$ are proportional to lattice energy parameters $\varepsilon_2$ and $\varepsilon_3$ (in table 3) in a certain way, although their scale factors are unequal. So $\sigma_2$ is positive and $\sigma_3$ is negative.

As we have mentioned in section 3, $b_\perp$ and $\gamma_0$ (misfit across interface) are in the same $\pm$. From (9), $\delta\gamma$ and $\gamma_0$ are on opposite $\pm$.

Then, substituting (11) into (10), we get

$$e_{dis} = \frac{1}{\rho}\sigma_2\int_S \delta\gamma^2 \, dS + \frac{1}{\rho}\sigma_3\int_S \delta\gamma^3 \, dS. \tag{12}$$

As $\sigma_2 > 0$ and $\sigma_3 < 0$, there are $\sigma_2\int_S \delta\gamma^2 \, dS > 0$ and $\sigma_3\int_S \delta\gamma^3 \, dS \gtrless 0$ at $\gamma_0 \gtrless 0$. Considering the two terms, $e_{dis}$ is always positive at $\gamma_0 > 0$, but can be negative at $\gamma_0 < 0$. The latter includes (Ag and Au)/$Al_2O_3$ interfaces.

Based on the above discussions, we are going to calculate dislocation density $\rho$. Just like for dislocation position, it is also determined by the lowest energy principle. From (3), the total energy is

$$E_{total} = S(\rho e_{dis} + \sigma_{M/Al_2O_3} + \sigma) + n\varepsilon. \tag{13}$$

In principle, the target $\rho$ is obtained at $\min\{E_{total}\}$, or in derivative form

$$\frac{d}{d\rho}E_{total} = 0. \tag{14}$$

For the derivation, let us use $L$ as the number of metal MLs and $\Delta S$ as the area per atom on the interface (which is

**Table 6.** The values of $\rho$, $\sigma'_{M/Al_2O_3}$ and $\theta$ at $L \to \infty$.

| | | $b$ | $\rho$ (Å$^{-1}$) | $\sigma'_{M/Al_2O_3}$ (eV Å$^{-2}$) | $\theta$ (deg) |
|---|---|---|---|---|---|
| $Ag/Al_2O_3$ | $b \perp$ DL | $\frac{a_M}{2}[1\bar{1}0]$ | 0.0421 | 0.0857 | — |
| | $b \not\perp$ DL | $\frac{a_M}{2}[1\bar{1}0]$ | 0.0486 | 0.1113 | 2.0381 |
| $Au/Al_2O_3$ | $b \perp$ DL | $\frac{a_M}{2}[1\bar{1}0]$ | 0.0459 | 0.1120 | — |
| | $b \not\perp$ DL | $\frac{a_M}{2}[1\bar{1}0]$ | 0.0530 | 0.1310 | 2.2401 |
| $Cu/Al_2O_3$ | $b \perp$ DL | $\frac{a_M}{6}[2\bar{1}\bar{1}]$ | 0.0967 | 0.2023 | — |
| | $b \not\perp$ DL | $\frac{a_M}{2}[1\bar{1}0]$ | 0.0645 | 0.0407 | 2.3692 |

equal to $\Delta S = \frac{a^2_{Al_2O_3}}{2\sqrt{3}} = 6.54$ Å$^2$). There is a relation

$$\frac{S}{n} = \frac{\Delta S}{L}. \tag{15}$$

Substituting (4)–(6) and (15) into (13), we get

$$\begin{aligned}\frac{\mathrm{d}}{\mathrm{d}\rho}E_{\text{total}} &= Se_{\text{dis}} + n\frac{\mathrm{d}\varepsilon}{\mathrm{d}\rho} \\ &= \frac{SL}{\Delta S}\left(3\varepsilon_3\gamma^2\frac{\mathrm{d}\gamma}{\mathrm{d}\rho} + 2\varepsilon_2\gamma\frac{\mathrm{d}\gamma}{\mathrm{d}\rho} + \frac{e_{\text{dis}}\Delta S}{L}\right) \\ &= \frac{SL}{\Delta S}\left(-\frac{3}{2}b_\perp\varepsilon_3\gamma^2 - b_\perp\varepsilon_2\gamma + \frac{e_{\text{dis}}\Delta S}{L}\right).\end{aligned} \tag{16}$$

Considering (14), a quadratic equation is obtained:

$$\frac{3}{2}b_\perp\varepsilon_3\gamma^2 + b_\perp\varepsilon_2\gamma - \frac{e_{\text{dis}}\Delta S}{L} = 0. \tag{17}$$

Note that $\rho$ does not appear in this equation. It is included in the residual misfit $\gamma$, as shown in (5). The method is to calculate $\gamma$ by (17) and calculate $\rho$ from $\gamma$ via (5).

By the way, (17) shows $\gamma$ is dependent on $L$. It means that dislocation density is dependent on the number of metal MLs. This is a very interesting result and needs more discussion.

First, let us pay attention to the ultimate condition at $L \to \infty$. In this case, (17) changes to

$$\tfrac{3}{2}b_\perp\varepsilon_3\gamma^2 + b_\perp\varepsilon_2\gamma = 0. \tag{18}$$

The reasonable solution is $\gamma = 0$, so $\rho = 2\frac{\gamma_0}{b_\perp}$. Generalized interface energy $\sigma'_{M/Al_2O_3}$ and epitaxial angle $\theta$ are also calculated, as listed in table 6.

Considering the values of $\sigma'_{M/Al_2O_3}$, the energy-preferred Burgers vector is $\frac{a_M}{2}[1\bar{1}0]$ for all three interfaces. The DN is hexagonal for (Ag and Au)/$Al_2O_3$ ($b \perp$ DL, figure 4(a.1)) and trigonal for $Cu/Al_2O_3$ ($b \not\perp$ DL, figure 4(b)). In particular, there is a small angle 2.3692° between $Cu[1\bar{1}0]$ and $Al_2O_3[11\bar{2}0]$.

However, table 6 is at $L \to \infty$, but the results about the Burgers vector and DN are not limited in this ultimate condition. A series of checks show that, for $L$ from 5 to 100 MLs, $b \perp$ DL is always preferred for (Ag and Au)/$Al_2O_3$ and $b \not\perp$ DL is preferred for $Cu/Al_2O_3$.

Next, we calculated $\rho$ at $L < \infty$, based on the above results. Figure 9 shows that the $\rho$ versus $L$ curves are descending for (Ag and Au)/$Al_2O_3$ and rising for $Cu/Al_2O_3$.

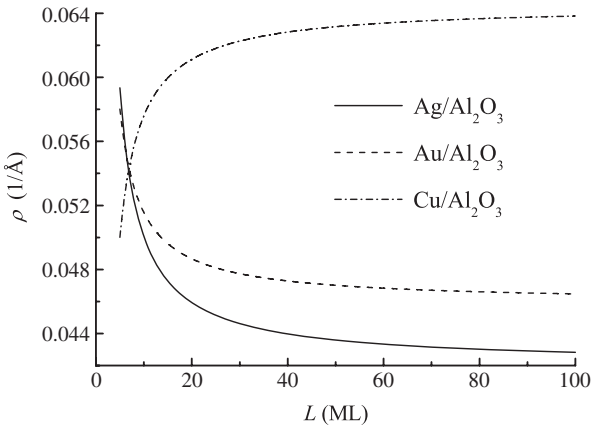


**Figure 9.** $\rho$ versus $L$ curves for (Ag, Au and Cu)/$Al_2O_3$ interfaces, at the energy-preferred Burgers vector and DN.

### *4.5. Discussion*

An important issue mentioned above is that dislocation energy is negative for (Ag and Au)/$Al_2O_3$. This originates from the third-order term in (11), related to the argument 'metals are easier to stretch than to compress'. It leads to some interesting results.

First, as we know, in most mismatch interfaces, there is a critical thickness for supported films. Below this thickness, the interface is coherent, without misfit dislocation. But for (Ag and Au)/$Al_2O_3$, we have proved that there is no such kind of critical thickness. The negative $e_{\text{dis}}$ calls for DLs, so even the metal film is quite thin.

Second, for (Ag and Au)/$Al_2O_3$, dislocation density is quite large if the metal film is thin enough (see figure 9). As $e_{\text{dis}}$ is negative, generalized interface energy $\sigma'_{M/Al_2O_3}$ ($=\sigma_{M/Al_2O_3} + \rho e_{\text{dis}}$, from (4)), is also negative at this condition. This is very interesting. Because interface energy is usually positive, to get the smallest interface area resulted in an interface plane. But $\sigma'_{M/Al_2O_3} < 0$ can destroy this plane, instead by a rough dentation structure. In our mind, this may be why Ag and Au films cannot grow epitaxially on $Al_2O_3$ in experiments.

## 5. Conclusion

In this work, we use the atomistic calculation method to study (Ag, Au and Cu)/$(Al_2O_3(0001))_{Al}$ interfaces. The purpose is to understand interface structure in 'atomic representation' and 'dislocation representation'. As a main advantage, we prove that the DN can give a reasonable description of the mismatch interface's structure. A series of interesting results is obtained.

First, all three interfaces have a mixed translation layer, consisting of a $\frac{1}{3}$ Al layer and $\frac{2}{3}$ metal layer.

Second, the DL is above this translation layer. Its Burgers vector is $\frac{a_M}{2}[1\bar{1}0]$. The DN is hexagonal in (Ag and Au)/$Al_2O_3$ ($b \perp$ DL) and trigonal in $Cu/Al_2O_3$ ($b \not\perp$ DL). In particular, there is a small angle 2.3692° between $Cu[1\bar{1}0]$ and $Al_2O_3[11\bar{2}0]$.

Third, dislocation energy is negative for (Ag and Au)/$Al_2O_3$ and positive for $Cu/Al_2O_3$. The former one can lead to

negative interface energy in some cases. At this condition, the interface area tends to enlarge, resulting in a rough dentation structure. This may be why Ag and Au epitaxial films have not been found on $Al_2O_3$(0001).

## Acknowledgments

This work is supported by the Nature Science Foundation of China (NSFC), no. 50531050 and the 973 Project, no. 2006CB605100.

## References

[1] Sanchez A, Abbet S, Heiz U, Schneider W D, Häkkinen H, Barnett R N and Landman U 1999 When gold is not noble: nanoscale gold catalysts *J. Phys. Chem.* A **103** 9573
[2] Fecht H J 1997 EPS industrial workshop: towards applications of nano- and quasi-crystalline materials *Europhys. News* **28** 89
[3] Padture N P, Gell M and Jordan E H 2002 Thermal barrier coatings for gas-turbine engine applications *Science* **296** 280
[4] Evans A G, Hutchinson J W and Wei Y 1999 Interface adhesion: effects of plasticity and segregation *Acta Mater.* **47** 4093
[5] Saiz E, Cannon R M and Tomsia A P 1999 Energetics and atomic transport at liquid metal/$Al_2O_3$ interfaces *Acta Mater.* **47** 4209
[6] Renaud G, Guénard P and Barbier A 1998 Misfit dislocation network at the Ag/MgO(001) interface: a grazing-incidence x-ray-scattering study *Phys. Rev.* B **58** 7310
[7] Renaud G and Barbier A 1999 Structure and morphology of the Pd/MgO(001) interface during its formation *Appl. Surf. Sci.* **142** 14
[8] Dmitriev S V, Yoshikawa N and Kagawa Y 2004 Misfit accommodation at the Cu(111)/$\alpha$-$Al_2O_3$ (0001) interface studied by atomistic simulation *Comput. Mater. Sci.* **29** 95
[9] Dmitriev S V, Yoshikawa N, Kohyama M, Tanaka S, Yang R and Kagawa Y 2004 Atomistic structure of the Cu(111)/a-$Al_2O_3$ (0001) interface in terms of interatomic potentials fitted to *ab initio* results *Acta Mater.* **52** 1959
[10] Shi S Q, Tanaka S and Kohyama M 2007 First-principles study of the tensile strength and failure of $\alpha$-$Al_2O_3$(0001)/Ni(111) interfaces *Phys. Rev.* B **76** 075431
[11] Shashkov D A, Chisholm M F and Seidman D N 1999 Atomic-scale structure and chemistry of ceramic/metal interfaces—I. Atomic structure of {222}MgO/Cu(Ag) interfaces *Acta Mater.* **47** 3939
[12] Shashkov D A, Muller D A and Seidman D N 1999 Atomic-scale structure and chemistry of ceramic/metal interfaces—II. Solute segregation at MgO/Cu(Ag) and CdO/Ag(Au) interfaces *Acta Mater.* **47** 3953
[13] Goniakowski J 1999 Transition metals on the MgO(100) surface: evolution of adsorption characteristics along the 4d series *Phys. Rev.* B **59** 11047
[14] Long Y and Chen N X 2007 Pair potential approach for metal/$Al_2O_3$ interface *J. Phys.: Condens. Matter* **19** 196216
[15] Long Y and Chen N X 2008 Interface reconstruction and dislocation networks for a metal/alumina interface: an atomistic approach *J. Phys.: Condens. Matter* **20** 135005
[16] Gutekunst G, Mayer J and Rühle M 1997 Atomic structure of epitaxial Nb-$Al_2O_3$ interfaces: I. Coherent regions *Phil. Mag.* A **75** 1329
[17] Gutekunst G, Mayer J, Vitek V and Rühle M 1997 Atomic structure of epitaxial Nb-$Al_2O_3$ interfaces: II. Misfit dislocations *Phil. Mag.* A **75** 1357
[18] Ernst F, Pirouz P and Heuer A H 1991 HRTEM study of a Cu/$Al_2O_3$ interface *Phil. Mag.* A **63** 259
[19] Dehm G, Scheu C, Rühle M and Raj R 1998 Growth and structure of internal Cu/$Al_2O_3$ and Cu/Ti/$Al_2O_3$ interfaces *Acta Mater.* **46** 759
[20] Zhukovskii Yu F, Kotomin E A, Herschend B, Hermansson K and Jacobs P W M 2002 The adhesion properties of the Ag/$\alpha$-$Al_2O_3$ (0001) interface: an *ab initio* study *Surf. Sci.* **513** 343
[21] Feng J W, Zhang W Q and Jiang W 2005 *Ab initio* study of Ag/$Al_2O_3$ and Au/$Al_2O_3$ interfaces *Phys. Rev.* B **72** 115423
[22] Smith J R and Zhang W 2000 Stoichiometric interfaces of Al and Ag with $Al_2O_3$ *Acta Mater.* **48** 4395
[23] Levy M, Bass H E and Stern R R (ed) 2001 *Handbook of Elastic Properties of Solids, Liquids and Gases* (San Diego, CA: Academic)
[24] Chen N X, Chen Z D, Shen Y N, Liu S J and Li M 1994 3D inverse lattice problems and Möbius-inversion *Phys. Lett.* A **184** 347
[25] Long Y, Chen N X and Zhang W Q 2005 Pair potentials for metal–ceramic interface by inversion of adhesive energy *J. Phys.: Condens. Matter* **17** 2045
[26] Zhao H Y and Chen N X 2008 An inverse adhesion problem for extracting interfacial pair potentials for the Al(001)/3C-SiC(001) interface *Inverse Probl.* **24** 035019
[27] Long Y and Chen N X 2008 An atomistic simulation and phenomenological approach of misfit dislocation in metal/oxide interfaces *Surf. Sci.* **602** 1122
[28] Accelrys Inc. 1999 *Cerius*$^2$ *4.0* software (Forcefield Engines)
[29] Ernst F 1995 Metal-oxide interfaces *Mater. Sci. Eng.* R **14** 97